

Facile Synthesis of Mesoporous SiO₂ Nanoparticles using the Mobility Differences of Etchants for Environmental Remediation

Yi Seul Lee, Gyo Yeon Byun, and Won San Choi

Abstract— In this paper, we report the preparation of mesoporous silica nanoparticles (MSNPs) using the mobility differences of sulfonate or sulfate-containing materials as etchants. The MSNPs were synthesised by treating silica nanoparticles (SNPs) with styrene sulfonate (SS) or sodium dodecyl sulfate (SDS) under heat. The simple treatment of the SNPs with SS or SDS led to surface etching of the SNPs, resulting in surface roughening and pore generation within the silica structure. The surface structuring of the SNPs could also be controlled by varying the concentration of counter ions of the etchants. This one-step process is very simple, facile, and scalable. The MSNPs appeared almost transparent in an aqueous solution due to their unique surface morphology. The resulting MSNPs also exhibited excellent adsorption and desorption properties for toxic organic pollutants.

Index Terms—About four key words or phrases in alphabetical order, separated by commas.

I. INTRODUCTION

Since the first reports on mesoporous silica nanoparticles (MSNPs) in the early 1990s, these materials have attracted continuous interest due to their unique properties, such as high specific surface areas, controllable pore structures, and narrow pore size distributions.^[1,2] Many synthetic protocols for preparing the MSNPs with controlled pore structures have been proposed. Among these methods, MSNPs are typically synthesised using a surfactant-templated technique that induces the formation of porous silica structures through the spontaneous co-assembly of the surfactants and inorganic precursors. This method generates well-ordered pore structures within the MSNPs. As a simpler approach, etching with an acid or base is also used to prepare MSNPs, which leads to the formation of random pore structures within the MSNPs. Although the resulting pore structure is not highly ordered, this technique possess the advantage of easily controlling the pore size and structures through simple tuning of the reaction conditions. Thus, diverse MSNPs have recently been created through the use of unique etching processes.

Silica-etching chemistry can be divided into two main

categories: 1) reversible etching in a hot aqueous solution of an acid or base and 2) irreversible etching in HF solution. With the former category, etching induces cleavage of the Si-O-Si bonds to form less-condensed oligomers of silica species. This bond cleavage can be reversed by the formation of bonds among diverse silicate oligomers. Regarding the latter category, etching by HF is a very rapid and irreversible process, and the primary product is gaseous silicon tetrafluoride (SiF₄). To date, the most common etchants used are NaOH, Na₂CO₃, and ammonia as bases and HCl and HF as acids, which exhibit different etching behaviours, as mentioned above. Therefore, from the perspective of the etching property of the etchant, there is a significant need to develop a new etchant for the facile and effective preparation of MSNPs with easily controlled pore structures. Herein, we report a facile method for the synthesis of MSNPs using the mobility differences of sulfonate or sulfate-containing materials as etchants. To the best of our knowledge, there have been no reports indicating that MSNPs can be created by SiO₂ etching using sulfur-containing etchants and their mobility differences.

II. EXPERIMENTAL SECTION

A. Materials

Tetraethyl orthosilicate (TEOS), ammonium hydroxide solution (NH₄OH), 2-propanol, sodium 4-vinylbenzenesulfonate (SS monomer), sodium dodecyl sulfate (SDS), acrylic acid (AA), poly(sodium 4-styrene sulfonate) (PSS, Mw: 70 000), sodium sulfate (Na₂SO₄), NaCl and methylene blue (MB) were purchased from Aldrich and used as received. Deionised (DI) water with a resistance of 18.2 MU cm was obtained using a Millipore Simplicity 185 system.

B. Synthesis of silica nanoparticles

An aqueous solution containing DI water (0.18 mL), 2-propanol (1 mL) and NH₄OH (0.03 mL) was prepared and stirred for 1 min. Then, 0.03 mL of TEOS was added to the resulting solution, followed by vigorous stirring for 30 min. After synthesis of the silica nanoparticles, the resulting solution was washed 3 times with DI water and stored as a solution by dispersing it into 1.2 mL of DI water. This synthetic scheme was found to be scalable up to 100 times the reactant amount. Preparation of SS-treated mesoporous silica particle (SS-MS) A total of 0.6 g of SS monomer was completely dissolved in 7 mL of DI water. To this solution, the suspension of silica nanoparticles (1.5 mL) was added and stirred for 24 h at 80 C. The opaque white-coloured solution

F. A. Author is with the National Institute of Standards and Technology, Boulder, CO 80305 USA (e-mail: author@boulder.nist.gov).

S. B. Author was with Rice University, Houston, TX 77005 USA. He is now with the Department of Physics, Colorado State University, Fort Collins, CO 80523 USA (e-mail: author@lamar.colostate.edu).

T. C. Author is with the Electrical Engineering Department, University of Colorado, Boulder, CO 80309 USA, on leave from the National Research Institute for Metals, Tsukuba, Japan (e-mail: author@nrim.go.jp).

changed to a clear solution as the reaction with the SS monomer proceeded. After reaction with the SS monomer, the resulting suspension of mesoporous silica was washed 3 times by centrifugation at 17 000 rpm for 1 min and redispersed in DI water. SDS can also be used for the preparation of mesoporous silica with a similar reaction setup using an aqueous solution of SDS with the same molar concentration rather than the SS monomer. For comparison, PSS, AA, and Na₂SO₄ with the same molar concentration were used. NaCl (0.5 M) was used to investigate the influence of counter ions of the etchant in the sulfonate on the surface structuring of the SNPs.

III. RESULTS AND DISCUSSION

The experimental scheme for the preparation of MSNPs is presented in Fig. 1. Silica nanoparticles (SNPs) could be transformed into MSNPs through a simple one-step reaction with styrene sulfonate (SS) monomers under heat treatment at 80 °C. The SS monomers, which served as an oxidising agent, gradually etched the SiO₂ surface due to their high oxidising potential. Additionally, they were embedded into the silica surface during formation of the MSNPs because the SS monomer possessed appropriate mobility that can moderately etch the SNPs.



Fig. 1. Schematic illustration of the formation of mesoporous SiO₂ nanoparticles by treatment with SS monomer.

Fig. 2 shows field-emission electron microscopy (FE-SEM) images of the SNPs before and after treatment with SS monomers at 80 °C. The bare SNPs with an average size of 210 nm exhibited a smooth surface morphology (Fig. 2a). After treatment with SS monomers, the surface of the SNPs was gradually etched from the edge to the centre of the SNPs, and the roughness of the surface increased as the reaction with the SS monomer proceeded (Fig. 2b–e). Tiny bumpy structures were formed on the SNPs during the early stage of the reaction, and these structures grew into irregular bumpy structures with a size of 30–60 nm, leading to the formation of porous SNPs. The average size of the resulting porous particles decreased to 75% of that of the original SNPs with increasing reaction time (Fig. S1a and b†). In the absence of SS monomer, the etching process of the SNPs did not occur (Fig. S1c†). The specific surface area and pore size of the SNPs after treatment with SS monomers were investigated using Brunauer–Emmett–Teller (BET) and Barrett–Joyner–Halenda (BJH) measurements. The nitrogen adsorption–desorption isotherm curve of the resulting particles exhibited a typical mesoporous type (Fig. 2f). Most of the pores were within the range of 2–20 nm. From the BJH measurements, the average pore size was determined to be 18 nm. The BET specific surface area and the BJH desorption cumulative pore volume (VP) were 71.8 m² g⁻¹ and 0.29 cm³

g⁻¹, respectively.

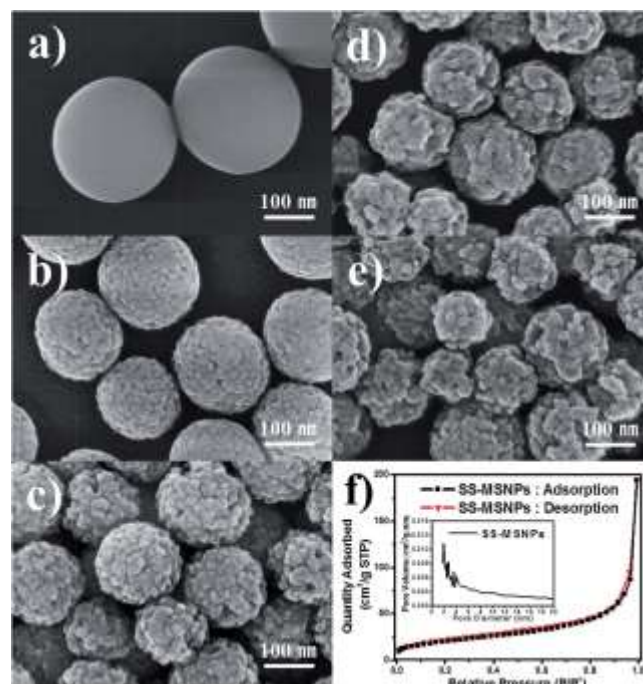


Fig. 2 SEM images of the SNPs (a) before and (b–e) after treatment with the SS monomer at 80 °C for (a) 0 h, (b) 1 h, (c) 6 h, (d) 12 h, and (e) 24 h. (f) BET and BJH data of e.

Because peroxymonosulfate (PMS), a type of (bi)sulfate/fate (SO₃/SO₄), has a higher oxidising potential (1.82 eV) than H₂O₂ (1.76 eV),^{31–33} this result is likely due to the etching of the SNP surface caused by the reaction of SiO₂ with sulfonates of the SS monomer. The surface chemistry of the MSNPs after reaction with the SS monomer was investigated using X-ray photoelectron spectroscopy (XPS) and Fourier transform-infrared (FT-IR) spectroscopy. Fig. 3a presents the XPS survey spectrum of the MSNPs, which clearly shows C and S compositions that are not observed in the bare SNPs. Fig. 3b presents the C 1s spectrum. The peak centred at 285 eV corresponds to methylene carbons or carbon bound to sulfur.³³ The S 2p spectrum at 167 eV also reveals presence of the sulfonate groups of the SS monomer (Fig. 3c). After reaction with SS monomers, new aliphatic CH and asymmetric SO₂ stretching bands, which are not observed in the bare SNPs, were also detected at 2950 and 1360 cm⁻¹, respectively (Fig. 3d, red line). These results suggest that the negatively charged SS monomers are chemisorbed on the negatively charged SiO₂ during the formation of the MSNPs.

The surface charge of the MSNPs was $z \pm 91.3$ mV, which was remarkably increased compared to that of the SNPs ($z \pm 65.6$ mV) before reaction with SS (Fig. S2†). The treatment of the SNPs with SS monomers changed the surface charge of the SNPs from negative to more negative, indicating exposure of surface area or impregnation of SS monomers. From the XPS, FT-IR, and zeta potential results, we conclude that the sulfonates of the SS, which served as an oxidising agent, gradually etched the SiO₂ surface due to their high oxidising potential and that they were embedded in the silica surface during the formation of MSNPs.

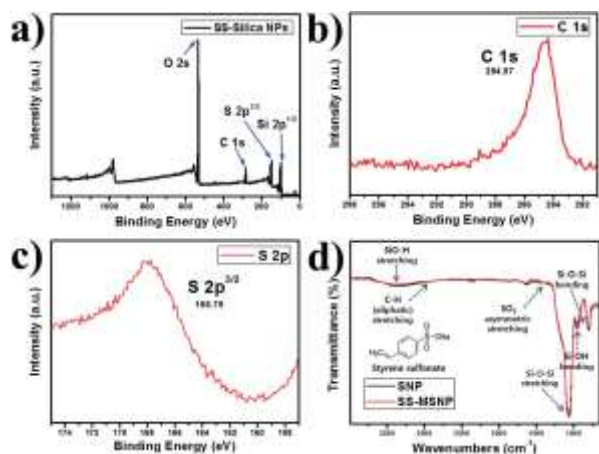


Fig. 3 (ac) XPS spectra and (d) FTIR spectra of SNPs after SS treatment (a) Survey (b) C 1s core level and (c) S 2p core level.

To further investigate the role of the sulfonates, we conducted control experiments using several materials that contain sulfonate or sulfate groups in their structure as a comparative study. Fig. S3† presents SEM images of SNPs treated with sodium sulfate (Na_2SO_4), poly(4-styrene sulfonate) (PSS), sodium dodecyl sulfate (SDS), and acrylic acid (AA). To compare performance of the possible etchant materials, we used same molar concentration of the etchants while other experimental conditions remained unchanged. In the case of Na_2SO_4 , most of the SNPs could not be detected by SEM analyses, indicating that a considerable amount of the SNPs was etched and removed under the same conditions compared to the MSNPs and bare SNPs (Fig. S3a and b†). Notably, in the case of PSS, the SNPs were very slightly etched, and their size was almost unchanged despite the presence of sulfonate groups on the PSS (Fig. S3c†). However, the treatment of the SNPs with SDS resulted in the formation of porous SNPs, which are very similar to the MSNPs prepared by reaction with the SS monomer (Fig. S3d†). The SNPs became porous SNPs through a similar etching process as the reaction with SDS proceeded (Fig. S3e–g†). The MSNPs generated from the reaction with SDS also showed similar XPS and FT-IR results as the MSNPs obtained from the SS monomer, thereby confirming that SDS is also embedded in the MSNPs (Fig. S4†). In the case of the etching with AA possessing negative charges, no detectable structural changes of the silica surface were observed (Fig. S3h†), indicating that the formation of the MSNPs is attributed to the reaction of SiO_2 with a specific type of functional group, such as sulfate or sulfonate (SO_3/SO_4). In summary, under the same conditions, small molecules such as Na_2SO_4 etched the SNPs considerably more than did large molecules such as PSS. This result may have occurred because the small-sized molecules can easily etch the SNPs due to their high mobility or degree of rotational freedom compared to large-sized molecules with a relatively low mobility. Additionally, the SS monomer and SDS possess relatively similar structures, such as hydrophilic head (sulfonate/sulfate) and hydrophobic tail (bulky alkyl) groups. They are also relatively similar in size compared with PSS and Na_2SO_4 . Thus, we hypothesize that the SS monomers and SDS possessing appropriate mobilities moderately etch the SNPs, not too strong or weak, to form MSNPs. We believe

that use of SS or SDS etchant for generation of MSNPs have several advantages over other reported methods for the following reasons: (i) no surface treatment is necessary to provide functionality of the MSNPs.

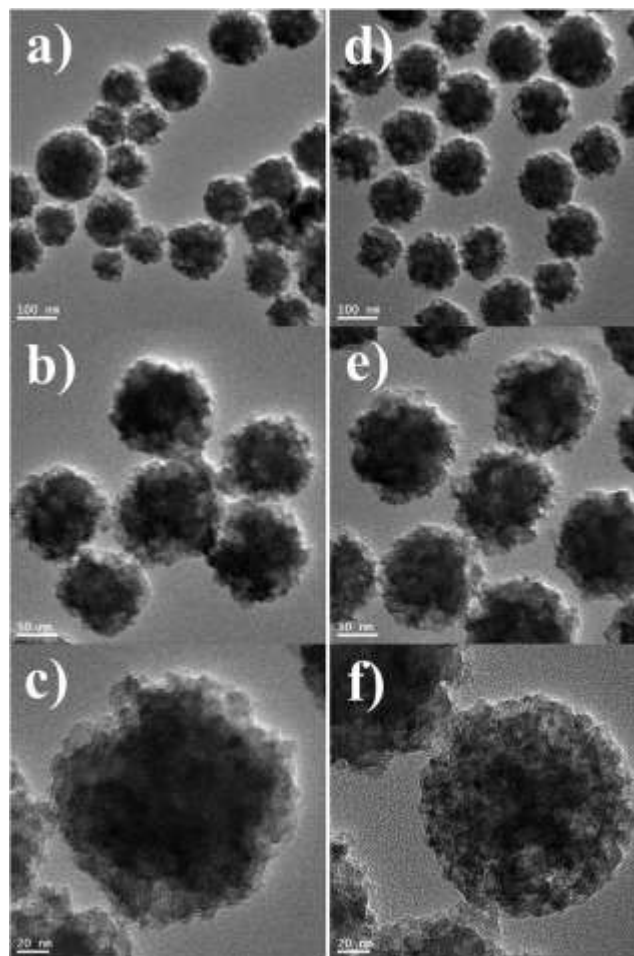


Fig. 4 TEM images of MSNPs obtained from (a–c) SS and (d–f) SDS treatments.

Surface treatment with sulfonate or sulfate groups can simultaneously be completed during the etching of SiO_2 with the SS or SDS, respectively. The SS treatment can also provide better dispersion of the MSNPs by providing a stable negative surface charge benefited from the presence of the SS. In general, use of typical methods need additional surface treatment for providing functionality and stable dispersions either during or after the process.17–23 (ii) The SiO_2 surface only can be etched by SS treatment, which can be used for selective etching of SiO_2 surface. Previous reported treatments result in the surface etching as well as internal etching of SiO_2 simultaneously.11,27,34–36 (iii) The SS is relatively less toxic compared to HCl, HF, or NaOH, thus it could be one of new etchants for the facile and effective preparation of MSNPs with easily controllable pore structures.

To clarify why the MSNPs appeared almost transparent, the internal structure of the MSNPs treated with the SS monomer or SDS was investigated using field-emission transmission electron microscopy (FE-TEM). As a common feature of the MSNPs obtained from the reaction with the SS monomer or SDS, the TEM images reveal the development of

randomly distributed pores within the silica structure and a low density at the particle edges (Fig. 4). The average sizes of both cases were almost similar at 154 nm. Considering the SEM and TEM results, it can be concluded that pores and tiny bumps are formed on the SNP surface through the random etching of SNPs, leading to the formation of hierarchical structures of several tens of nanometre-sized pore structures within the several hundred nanometre-sized MSNP structures. This kind of structure was prepared upon reaction time for 24 h, and interestingly, prolonged reaction doesn't induce larger cavities in their interior.³⁷ UV-vis transmittance spectra of the MSNPs obtained from the SS monomer treatment were analysed to obtain further insights.

We believe that our MSNPs can be used for variety of applications due to their porous structures and highly negative charges. As a quick demonstration, we tested the MSNPs for the efficient removal of toxic organic dyes, such as methylene blue (MB), from wastewater. Fig. 5a presents UV-vis spectra of the MB solution before and after treatment with the MSNPs. Prior to treatment with the MSNPs, the MB absorbance was strong (black line). After the removal process, the MB absorbance decreased significantly (red to bluish green). After the adsorption tests, the blue colour of the MB solution became transparent. In the 1st cycle, the removal of the MB was completed in 1 minute, which revealed the fast adsorption performance of the MSNPs for the removal of MB from water (Fig. 5b). The maximum adsorption capacity of the MSNPs for MB was determined to be 75.1 mg g⁻¹, which was calculated based on the absorbance ratio and molar absorption coefficient of MB using Beer-Lambert's Law. Basically, negatively charged silica and the SS have electrostatic interaction with positively charged MB molecules. The very high negative charge ($z \approx 91.3$ mV) and high surface area (71.8 m² g⁻¹) of the MSNPs can be considered one of the main reasons for the high adsorption of MB. The regeneration performance of the adsorbent is an important factor for practical applications. The development of a recyclable agent for the removal of toxic pollutants should involve reversible adsorption/desorption of the molecules by external stimuli. To investigate the desorption ability of the MSNPs, the concentration of MB released from the MSNPs with adsorbed MB (MSNP-MBs) using salt treatment was measured (Fig. 5c and d). SS and hydroxyl groups anchored on the MSNPs enabled the MB molecules to be easily adsorbed using electrostatic interactions and hydrogen bonding, and exposure to salt solution resulted in desorption of the MB molecules. Fig. 5c presents time-dependent UV-vis spectra of the MB solution desorbed from the MSNP-MBs. The absorbance at 664 nm increased as time increased, indicating that the concentration of MB gradually increased due to the release of MB from the MSNP-MBs. The MSNP-MB initially exhibited a burst-release of adsorbed MB within 1 min. The rapid release of MB from the MSNP-MB can be attributed to the MB molecules being adsorbed on the external surfaces of the MSNPs. Totals of 37.6% and 68.2% of the adsorbed MB were released over long periods of 12 h and 60 h, respectively, from the MSNP-MB, showing sustained release behaviour (Fig. 6d and S7†). This result could be explained by the

formation of hydrogen bonds between the $-N(CH_3)_2$ groups of MB and the $-SO_3$ groups of SS as well as the $-OH$ groups of SiO₂ inside the pore walls of the MSNPs, which holds back the release of the MB. These results suggest that the MSNPs described here may also be a promising candidate for drug delivery systems. Furthermore, calcined MSNPs were also tested for the removal of MB (Fig. 5e and f). The removal performances are maintained without deterioration, even after calcination. As a representative case, the result for the removal of MB was 95.4 mg g⁻¹, which was increased compared to that of the MSNPs prior to calcination (75.1 mg g⁻¹). This result can be attributed to the elimination of SS molecules embedded in the MSNPs after calcination, leading to an increase in the surface area of the MSNPs.

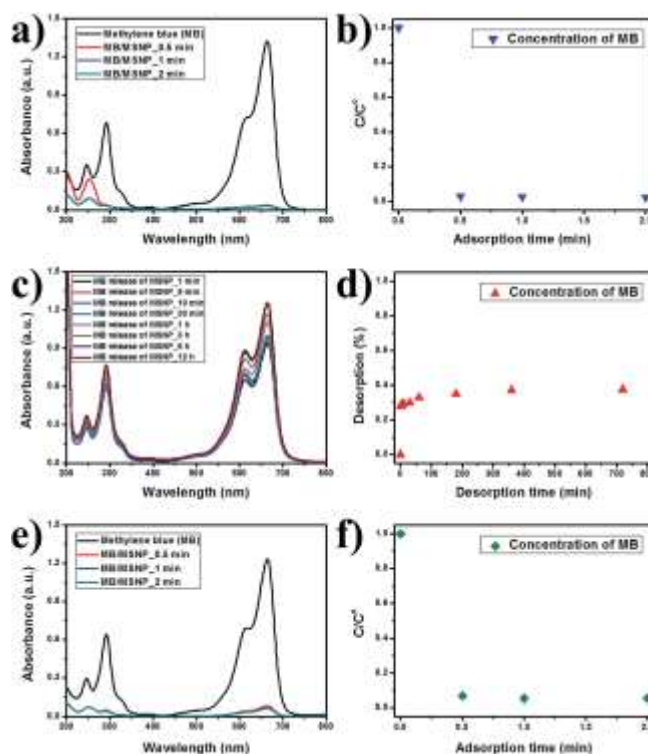


Fig. 5 (a and b) Adsorption test. (a) UV-vis absorption spectra of the MB solution before and after treatment with the MSNPs. (b) Adsorption rate of MB on the MSNPs. (c and d) Desorption test. (c) UV-vis absorption spectra of the MB released from the MSNP-MB as a function of increasing reaction time. (d) Percent desorption (1 min to 12 h, 1st step) of MB released from the MSNP-MB in a 0.5 M NaCl solution. (e and f) Adsorption test of calcined MSNPs. (e) UV-vis absorption spectra of the MB solution before and after treatment with calcined MSNPs. (f) Adsorption rate of MB on the calcined MSNPs

IV. CONCLUSION

In conclusion, we demonstrated a novel process for the synthesis of MSNPs, which were prepared by treating SNPs with SS monomer. The simple treatment of SNPs using SS or SDS as an etchant led to surface etching of the SNPs, resulting in surface roughening and pore generation within the silica structure. The etchant molecules that possessed relatively similar structures, such as hydrophilic head (sulfonate/sulfate) and hydrophobic tail (bulky alkyl) groups, appropriately etched the SNPs due to their moderate mobility or degree of rotational freedom, compared to large- or small-sized

molecules with a relatively too low or high mobility, respectively. The surface structuring of the SNPs could be controlled by varying the concentration of counter ions in the etchants used. The distinctive surface features of the MSNPs made the MSNPs almost transparent in aqueous solution. SS and hydroxyl groups anchored on the MSNPs enabled toxic organic groups to be easily adsorbed, and exposure to a salt solution resulted in desorption of the toxic organic groups. Furthermore, increased performance for the removal of pollutants was observed after calcination of the MSNPs. Thus, our MSNPs exhibited excellent removal ability and recyclability. This one-step process is very simple, facile, and scalable. We expect that our strategy can be extended to the facile synthesis of other transparent polymer nanocomposites based on transparent polymers and drug delivery carriers.

V. ACKNOWLEDGEMENTS

This research was supported by the Basic Science Research Program of the National Research Foundation of Korea (NRF) funded by the Ministry of Science, ICT & Future Planning (2014003515)

REFERENCES

(Periodical style)

- [1] C. T. Kresge, M. E. Leonowicz, W. J. Roth, J. C. Vartuli and J. S. Beck, *Nature*, 1992, 359, 710–712.
- [2] J. Y. Ying, C. P. Mehnert and M. S. Wong, *Angew. Chem., Int. Ed.*, 1999, 38, 56–77.
- [3] F. Hoffmann, M. Cornelius, J. Morell and M. Froba, *Angew. Chem., Int. Ed.*, 2006, 45, 3216–3251.
- [4] X. Du and J. He, *Nanoscale*, 2011, 3, 3984–4002.
- [5] Y. Chen, H.-R. Chen and J.-L. Shi, *Acc. Chem. Res.*, 2014, 47, 125–137.
- [6] S. H. Wu, C.-Y. Mou and H.-P. Lin, *Chem. Soc. Rev.*, 2013, 42, 3862–3875.
- [7] D. J. Mihalcik and W. Lin, *ChemCatChem*, 2009, 1, 406–413.
- [8] Y. Huang, W. Deng, E. Guo, P.-W. Chung, S. Chen, B. G. Trewyn, R. C. Brown and V. S.-Y. Lin, *ChemCatChem*, 2012, 4, 674–680.
- [9] X. Fang, X. Zhao, W. Fang, C. Chen and N. Zheng, *Nanoscale*, 2013, 5, 2205–2218.
- [10] L. Zhang, W. Zhang, J. Shi, Z. Hua, Y. Li and J. Yan, *Chem. Commun.*, 2003, 2, 210–211.
- [11] F. Tang, L. Li and D. Chen, *Adv. Mater.*, 2012, 24, 1504–1534.
- [12] Z. Li, J. C. Barnes, A. Bosoy, J. F. Stoddart and J. I. Zink, *Chem. Soc. Rev.*, 2012, 41, 2590–2605.
- [13] Y. Chen, P. Xu, H. Chen, Y. Li, W. Bu, Z. Shu, Y. Li, J. Zhang, L. Zhang, L. Pan, X. Cui, Z. Hua, J. Wang, L. Zhang and J. Shi, *Adv. Mater.*, 2013, 25, 3100–3105.
- [14] Y. Chen, Y. Gao, H. Chen, D. Zeng, Y. Li, Y. Zheng, F. Li, X. Ji, X. Wang, F. Chen, Q. He, L. Zhang and J. Shi, *Adv. Funct. Mater.*, 2012, 22, 1586–1597.
- [15] C. J. Brinker, *Curr. Opin. Solid State Mater. Sci.*, 1996, 1, 798–805.
- [16] N. K. Raman, M. T. Anderson and C. J. Brinker, *Chem. Mater.*, 1996, 8, 1682–1701.
- [17] V. Polshettiwar, D. Cha, X. Zhang and J. M. Basset, *Angew. Chem., Int. Ed.*, 2010, 49, 9652–9656.
- [18] J. Wu, Y. J. Zhu, S. W. Cao and F. Chen, *Adv. Mater.*, 2010, 22, 749–753.
- [19] Q. Ji, S. Acharya, P. J. Hill, A. Vinu, S. B. Yoon, J. Yu, K. Sakamoto and K. Ariga, *Adv. Funct. Mater.*, 2009, 19, 1792–1799.
- [20] T. Shiomi, T. Tsunoda, A. Kawai, S.-I. Matsuura, F. Mizukami and K. Sakaguchi, *Small*, 2009, 5, 67–71.
- [21] H. Kassab, M. Maksoud, S. Aguado, M. Pera-Titus, B. Albela and L. Bonnevot, *RSC Adv.*, 2012, 2, 2508–2516.
- [22] M. Liong, J. Lu, M. Kovichich, T. Xia, S. G. Ruehm, A. E. Nel, F. Tamanoi and J. I. Zink, *ACS Nano*, 2008, 2, 889–896.
- [23] D. K. Yi, S. S. Lee, G. C. Papae · hymiou and J. Y. Ying, *Chem. Mater.*, 2006, 18, 614–619S.
- [24] Q. Zhang, J. Ge, J. Goebl, Y. Hu, Z. Lu and Y. Yin, *Nano Res.*, 2009, 2, 583–591.
- [25] C.-C. Huang, W. Huang and C.-S. Yeh, *Biomaterials*, 2011, 32, 556–564.
- [26] D. Chen, L. Li, F. Tang and S. Qi, *Adv. Mater.*, 2009, 21, 3804–3807.
- [27] Q. Zhang, T. R. Zhang, J. P. Ge and Y. D. Yin, *Nano Lett.*, 2008, 8, 2867–2871.
- [28] T. R. Zhang, J. P. Ge, Y. X. Hu, Q. Zhang, S. Aloni and Y. D. Yin, *Angew. Chem., Int. Ed.*, 2008, 47, 5806–5811.
- [29] Y. S. Lin, S. H. Wu, C. T. Tseng, Y. Hung, C. Chang and C. Y. Mou, *Chem. Commun.*, 2009, 24, 3542–3544.
- [30] S. H. Wu, C. T. Tseng, Y. S. Lin, C. H. Lin, Y. Hung and C. Y. Mou, *J. Mater. Chem.*, 2011, 21, 789–794.
- [31] P. R. Shukla, S. Wang, H. Sun, H. M. Ang and M. Tad'e, *Appl. Catal., B*, 2010, 100, 529–534.
- [32] G. B. Lente, J. Z. Kalm'ar, Z. Baranyai, A. Z. Kun, I. K'ek, D. V. Bajusz, M. Tak'acs, L. Veres and I. N. F'abi'an, *Inorg. Chem.*, 2009, 48, 1763–1773.
- [33] J. Singh and J. E. Whitten, *J. Phys. Chem. C*, 2008, 112, 19088–19096.
- [34] S.-J. Park, Y.-J. Kim and S.-J. Park, *Langmuir*, 2008, 24, 12134–12137.
- [35] Q. Yu, P. Wang, S. Hu, J. Hui, J. Zhuang and X. Wang, *Langmuir*, 2011, 27, 7185–7191.
- [36] Y. J. Wong, L. Zhu, W. S. Teo, Y. W. Tan, Y. Yang, C. Wang and H. Chen, *J. Am. Chem. Soc.*, 2011, 133, 11422–11425.
- [37] Q. Wu, C. Liu, L. Fan, J. Shi, H. Jia, Q. Qi, L. Sun and F. Chen, *RSC Adv.*, 2013, 3, 7486–7494.
- [38] H. Y. Koo, D. K. Yi, S. J. Yoo and D.-Y. Kim, *Adv. Mater.*, 2004, 16, 274–277.
- [39] C. Aydin, A. Zaslavsky, G. J. Sonek and J. Goldstein, *Appl. Phys. Lett.*, 2002, 80, 2242–2244.
- [40] A. Gombert, W. Glaubit, K. Rose, J. Dreibholz, B. Blasi, A. Heinzl, D. Sporn, W. Doil and V. Wittwer, *Thin Solid Films*, 1999, 351, 73–78

All authors should include biographies with photo at the end of regular papers.)



Prof. Won San Choi received his PhD in materials science and engineering from Gwangju Institute of Science and Technology (GIST) in 2008. After his postdoctoral fellowship at University of Cambridge, Dept. of Chemistry, he joined Korea Basic Science Institute (KBSI). He moved the Hanbat National University as an associate professor since 2011. He has published over 50 journal papers, and his current research focuses on synthesis of nanomaterials for environmental remediation.